Introduction to Floquet theory

Konrad Viebahn*
Institute for Quantum Electronics, ETH Zurich, 8093 Zurich, Switzerland
(Dated: November 13, 2020)

These are introductory lecture notes on Floquet theory for applications in quantum optics and ultracold quantum gases, with a particular focus on driven optical lattices.

Floquet theory aims at finding solutions to the time-dependent Schrödinger equation with a time-periodic Hamiltonian:

$$i\hbar\frac{\mathrm{d}}{\mathrm{d}\tau}\left|\psi(\tau)\right\rangle = \mathcal{H}(\tau)\left|\psi(\tau)\right\rangle \tag{1}$$

$$\text{with}\quad \mathcal{H}(\tau) = \mathcal{H}(\tau+T)\ . \tag{2}$$

Analogies between Bloch theory and Floquet theory

Before we tackle the time-dependent problem, let us review briefly the theory describing spatially periodic, but temporally static systems: Bloch theory. There are some similarities between Floquet and Bloch theory that can help us gain an intuition on the former. For example, the real momentum p loses its meaning in Bloch theory and must be replaced by $\hbar q$, the *quasimomentum* $q \mod 2k_{\mathrm{lat}} = 2\pi/a$ (a is the lattice spacing), while in Floquet theory the energy becomes undefined and must be replaced by *quasienergy* $\mod \hbar\omega$, where $\omega = 2\pi/T$ is the driving frequency. Both theories reduce an originally intractable problem to a relevant low-energy subspace. However, the analogies between Bloch theory and Floquet theory only hold up to a certain point and should not be overstretched. One should keep in mind that the two descriptions are trying to solve two different problems. In Bloch theory, on the one hand, the underlying challenge is an infinite-dimensional Hamiltonian which can then be reduced to an approximate finite-dimensional one. In Floquet theory, on the other hand, the underlying challenge is the evaluation of a time-ordered integral (the time-evolution operator) which then turns out to be separable into slow-moving and fast-moving parts. This is independent of the dimension of the Hamiltonian: as we will see, it applies both to a two-level system and an extended optical lattice.

I. BLOCH'S THEOREM

Here, we are trying to find solutions to the stationary Schrödinger equation for a Hamiltonian with a spatially periodic potential

$$V(x) = V(x+a)\ , \tag{3}$$

where a is the lattice spacing. Bloch's theorem tells us that the solutions to Eq. 3 are of the form

$$\psi^n(x,q) = u^n(x,q)\times e^{iqx} \tag{4}$$

$$\text{with } u^n(x,q) = u^n(x+a,q)\ , \tag{5}$$

where $\psi^n(x,q)$ is sometimes called *Bloch wave* and $u^n(x,q)$ is called *Bloch function*. The argument q is called quasimomentum or lattice momentum and n labels the eigenstate (also called *band index*). At first sight, we have not gained anything but simply shifted the problem of finding $\psi^n(x,q)$ to another unknown function $u^n(x,q)$. However, the crucial advantage of the Bloch function is its periodicity (Eq. 5) which allows us to Fourier-expand it into position-independent coefficients $c_l^n(q)$:

$$u^n(x,q) = \sum_{l=-\infty}^{+\infty} c_l^n(q)e^{i2k_{\mathrm{lat}}lx} \tag{6}$$

$$\Rightarrow \psi^n(x,q) = \sum_{l=-\infty}^{+\infty} c_l^n(q)e^{i(2k_{\mathrm{lat}}l+q)x}\ . \tag{7}$$

We can now re-write the Hamiltonian resulting from Eq. 3 in the basis of plane waves (with the coefficients $c_l^n(q)$) which form the natural basis for spatially periodic problems.

Optical lattices

Let us directly look at an optical lattice as an example. The potential is given by

$$V(x) = V_0\cos^2(k_{\mathrm{lat}}x)\ . \tag{8}$$

You showed in a previous exercise that, using Eq. 7, the Hamiltonian can be written as

$$\mathcal{H}_{l,l'} = \begin{cases} \frac{\hbar^2}{2m}(q+2lk_{\mathrm{lat}})^2 & \text{for}\quad l=l' \\ V_0/4 & \text{for}\quad |l-l'|=1 \\ 0 & \text{otherwise,}\end{cases} \tag{9}$$

neglecting any static energy offsets. While this Hamiltonian is still infinite-dimensional, and hence intractable, the natural basis of plane waves allows us to truncate it at finite $\pm l_{\mathrm{max}}$, still capturing the proper low-energy behaviour. The matrix in Eq. 9 is sparse and can easily be diagonalised numerically to yield the well-known bandstructure (Fig. 1).

* viebahnk@phys.ethz.ch

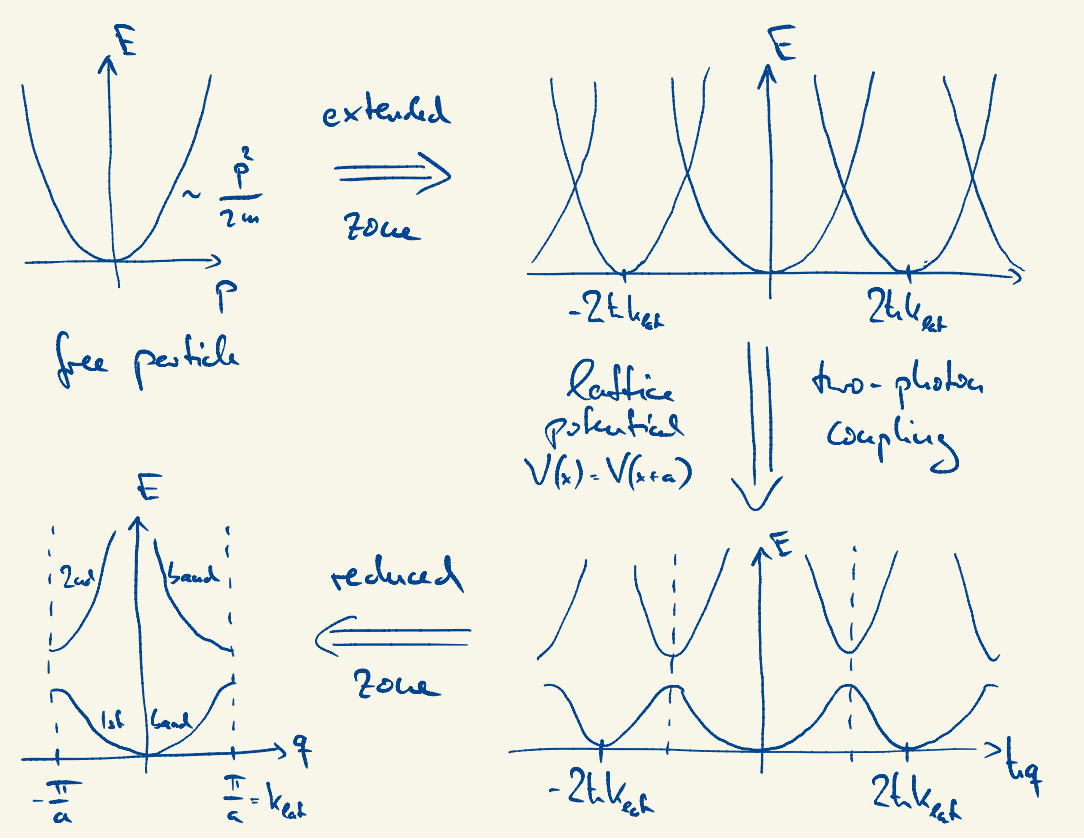

FIG. 1. Band structure of an optical lattice. By drawing free-particle dispersions separated by $2\hbar k_{\mathrm{lat}}$ and introducing a coupling between them, the characteristic band structure emerges. This description can then be reduced to a single Brillouin-zone with $q \in [-\frac{\pi}{a}, \frac{\pi}{a}]$.

The photon picture

An intuitive picture for the emergence of band gaps in the free-particle dispersion is the absorption and subsequent re-emission of a photon from the optical lattice. In a process in which the absorption and emission processes happen in opposite directions, the atom gets a momentum kick of $2\hbar k_{\mathrm{lat}}$, thereby coupling these states in the free-particle dispersion, leading to a gap opening. This picture is illustrated in Fig. 1 using 'extended zones'.

II. FLOQUET'S THEOREM

Now, let us get to the time-periodic problem, i.e.

$$\mathcal{U}(\tau_1, \tau_0) = \mathcal{T} \exp\left[-\frac{i}{\hbar}\int_{\tau_0}^{\tau_1} \mathcal{H}(\tau)\,\mathrm{d}\tau\right] \tag{10}$$

$$\text{with} \quad \mathcal{H}(\tau) = \mathcal{H}(\tau + T)\ . \tag{11}$$

($\mathcal{T}$ denotes time-ordering.) Here, a simple basis change à la Bloch or, equivalently, a change of reference frame will only work in specific situations, namely, if the stationary part of $\mathcal{H}(\tau)$ is rotationally invariant [1]. In these cases, the time-evolution can be completely absorbed into the rotating frame of reference. As we will see in an example, these situations can be understood as 'trivial' cases of Floquet theory, in which we do not rely on Floquet's theorem. The power of Floquet theory comes from the fact that, even if there remains a time-dependence in the rotating frame, we can still make the problem tractable using the periodicity of the Hamiltonian. In particular, we want to separate fast dynamics, within one period T of the Hamiltonian, from slow ones, which change from one period to the next.

Our derivation starts with noting the following ('semi-group') identity of the time-evolution operator (Eq. 10) that evolves a given state from an initial time τ_0 to $\tau_1+\tau_2$:

$$\mathcal{U}(\tau_1 + \tau_2, \tau_0) = \mathcal{U}(\tau_1 + \tau_2, \tau_1)\mathcal{U}(\tau_1, \tau_0)\ . \tag{12}$$

Now, for the periodically modulated Hamiltonian in Eq. 10, we have for the evolution from an initial time τ_0 to some final time $\tau + T$

$$\mathcal{U}(\tau + T, \tau_0) = \mathcal{U}(\tau + T, \tau_0 + T)\mathcal{U}(\tau_0 + T, \tau_0) \tag{13}$$

$$\overset{\text{Ex}}{=} \mathcal{U}(\tau, \tau_0)\mathcal{U}(\tau_0 + T, \tau_0)\ . \tag{14}$$

Now, knowing that any $\mathcal{U}(\tau_2, \tau_1)$ must be unitary (i.e. $\mathcal{U}^\dagger\mathcal{U} = \mathbb{1}$), we are able to write the second part

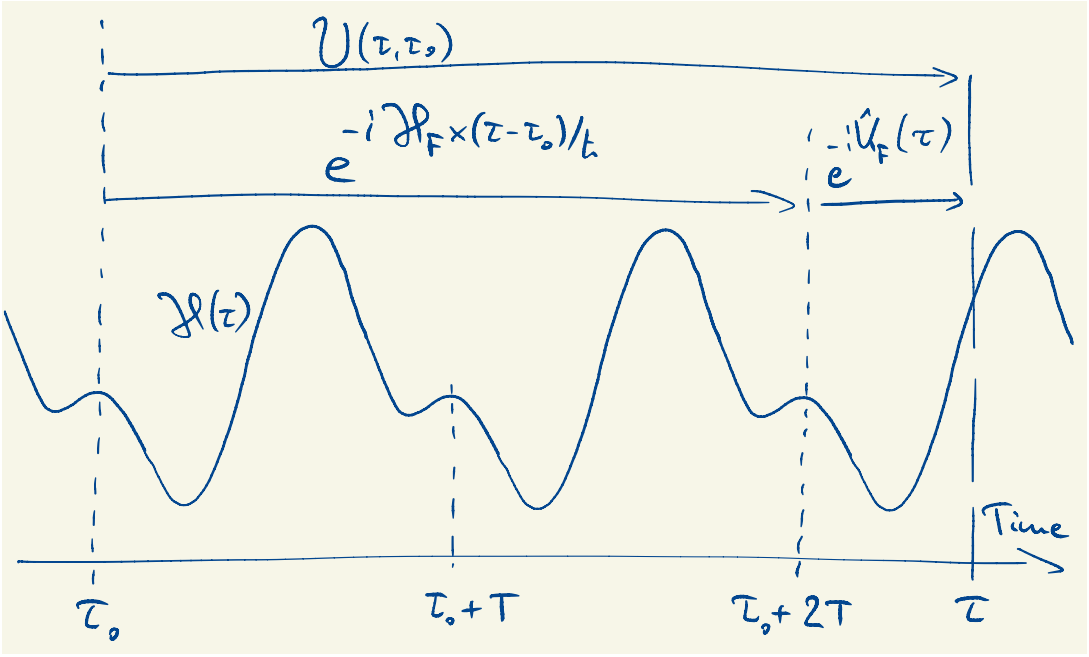

FIG. 2. Floquet's theorem illustrated. The slow dynamics (from one period T to the next) is captured by Floquet Hamiltonian $\mathcal{H}_{\rm F}$, whereas the fast 'micromotion' within a period is governed by the fast motion operator $e^{-i\hat{K}_{\rm F}(\tau)}$

.

of our time-evolution as

$$\mathcal{U}(\tau_0+T,\tau_0) \equiv e^{-i\mathcal{H}_{\rm F}\times T/\hbar}\ , \tag{15}$$

which defines $\mathcal{H}_{\rm F}$ as a time-independent, hermitian operator (i.e. $(\mathcal{H}_{\rm F})^\dagger = \mathcal{H}_{\rm F}$, ensuring that $\mathcal{U}(\tau_0+T,\tau_0)$ is unitary). The hermitian operator $\mathcal{H}_{\rm F}[\tau_0]$ does, in general, depend on the choice of initial time τ_0. With the help of Eq. 15 we define the 'fast-motion' operator

$$e^{-i\hat{K}_{\rm F}(\tau)} \equiv \mathcal{U}(\tau,\tau_0)e^{+i\mathcal{H}_{\rm F}\times(\tau-\tau_0)/\hbar}\ , \tag{16}$$

where $\hat{K}_{\rm F}(\tau)$ is called the 'stroboscopic kick operator' (for reasons that will hopefully become clear later). The fast-motion operator $e^{-i\hat{K}_{\rm F}(\tau)}$ obeys the following identity

$$\begin{aligned} e^{-i\hat{K}_{\rm F}(\tau+T)} &= \mathcal{U}(\tau+T,\tau_0)e^{+i\mathcal{H}_{\rm F}\times(\tau+T-\tau_0)/\hbar} \\ &\overset{(14)}{=} \mathcal{U}(\tau,\tau_0)\left(\mathcal{U}(\tau_0+T,\tau_0)e^{+i\mathcal{H}_{\rm F}\times T/\hbar}\right) \\ &\quad \times e^{+i\mathcal{H}_{\rm F}\times(\tau-\tau_0)/\hbar} \qquad (17) \\ &\overset{(15,16)}{=} e^{-i\hat{K}_{\rm F}(\tau)} \qquad (18) \end{aligned}$$

This means that the kick operator describes the motion within one period T but does not change from one period to the next (it just depends on the global choice of starting time τ_0). This allows us to directly write down Floquet's theorem for periodically modulated Hamiltonians:

$$\mathcal{U}(\tau,\tau_0) = e^{-i\hat{K}_{\rm F}(\tau)}e^{-i\mathcal{H}_{\rm F}\times(\tau-\tau_0)/\hbar} \tag{19}$$
$$\text{with} \qquad e^{-i\hat{K}_{\rm F}(\tau+T)} = e^{-i\hat{K}_{\rm F}(\tau)}\ .$$

This result is the mathematical way of separating the slow dynamics (governed by $\mathcal{H}_{\rm F}$) from the fast 'micromotion' during one period T (governed by $e^{-i\hat{K}_{\rm F}(\tau)}$), as illustrated in Fig. 2.

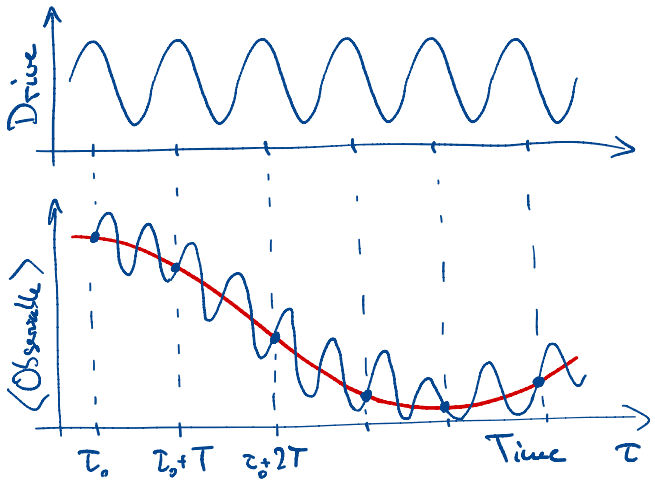

FIG. 3. The action of a periodic drive (upper panel) on the time-evolution of a quantum system. The slow dynamics of an observable (red line) is captured by the Floquet Hamiltonian $\mathcal{H}_{\rm F}$ whereas the exact dynamics (blue line) is composed of fast dynamics (micromotion) and slow dynamics. The micromotion is described by the kick operators $e^{-i\hat{K}_{\rm F}(\tau)}$ and vanishes at stroboscopic times τ_0, τ_0+T, etc (blue points).

In particular, we can now calculate the slow dynamics of a given quantum state over many periods T by simply evolving it with the static, hermitian operator $\mathcal{H}_\mathrm{F}$, as if it was a time-independent problem. For this reason, $\mathcal{H}_\mathrm{F}$ is called a 'Floquet Hamiltonian'. Keep in mind, however, that for reaching arbitrary final times τ (and also for arbitrary starting times $\tau_i \neq \tau_0$) we need to additionally apply the stroboscopic kick operator $\hat{K}_\mathrm{F}(\tau)$. At 'stroboscopic' times τ_0, $\tau_0 + T$, $\tau_0 + 2T$, etc. the kick operator is identically zero, which means

$$\begin{aligned} e^{-i\hat{K}_\mathrm{F}(\tau_0)} &= e^{-i\hat{K}_\mathrm{F}(\tau_0+T)} \\ &= e^{-i\hat{K}_\mathrm{F}(\tau_0+2T)} \\ &= \dots \\ &= \mathbb{1} \ . \end{aligned} \tag{20}$$

Consequently, the dynamics calculated by the Floquet Hamiltonian is exact at stroboscopic times, as illustrated in Fig. 3.

The Floquet gauge τ_0

So far, we have tacitly assumed a certain starting time τ_0 in all derivations. However, it is clear that the resulting dynamics will not be independent of the value of τ_0, as illustrated in Fig. 4. Indeed, both $\mathcal{H}_\mathrm{F}[\tau_0]$ and $\hat{K}_\mathrm{F}[\tau_0]$ carry an explicit dependence on τ_0 which will be denoted by the square brackets $[\cdot]$ throughout the text. What is the relevance of τ_0?

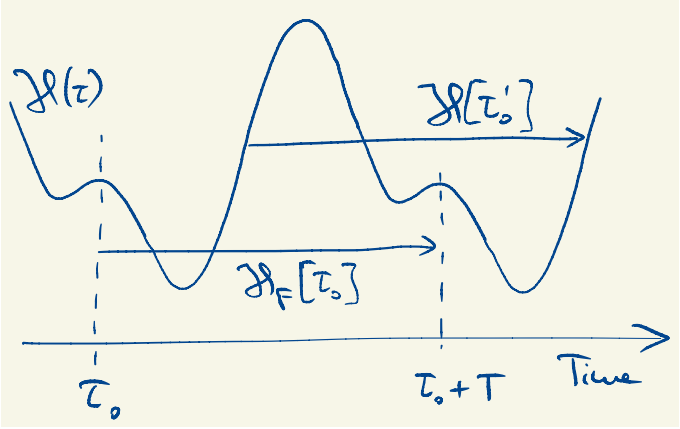

FIG. 4. The Floquet gauge τ_0. The Floquet Hamiltonian $\mathcal{H}_\mathrm{F}[\tau_0]$ depends on the choice of starting time. However, all Floquet Hamiltonians can be transformed into one another by a unitary transform (Eq. 21) and have the same spectrum. The micromotion will depend on the choice of starting time.

We note that all choices of τ_0 can be related via a unitary transformation:

$$\mathcal{H}_\mathrm{F}[\tau_0'] = \mathcal{U}(\tau_0', \tau_0)\mathcal{H}_\mathrm{F}[\tau_0]\mathcal{U}(\tau_0, \tau_0') \ . \tag{21}$$

(This is shown in ref. [1].) We can think of Eq. 21 as a gauge transformation and τ_0 as a gauge choice, called the 'Floquet gauge'. Hence, knowing one particular member of the family of Floquet Hamiltonians $\{\mathcal{H}_\mathrm{F}[\tau_0]\}$ allows us to reconstruct all other members. Correspondingly, the spectrum of $\mathcal{H}_\mathrm{F}[\tau_0]$ will not depend on τ_0.

Therefore, we should write the definition of the Floquet Hamiltonian and the stroboscopic kick operator with explicit τ_0 dependence as

$$\mathcal{U}(\tau_0 + T, \tau_0) = e^{-i\mathcal{H}_\mathrm{F}[\tau_0]\times T/\hbar} \tag{22}$$

$$e^{-i\hat{K}_\mathrm{F}[\tau_0](\tau)} = \mathcal{U}(\tau, \tau_0)e^{+i\mathcal{H}_\mathrm{F}[\tau_0]\times(\tau-\tau_0)/\hbar} \ , \tag{23}$$

leading to Floquet's theorem in its gauge-dependent form

$$\begin{aligned} \mathcal{U}(\tau, \tau_0) &= e^{-i\hat{K}_\mathrm{F}[\tau_0](\tau)}e^{-i\mathcal{H}_\mathrm{F}[\tau_0]\times(\tau-\tau_0)/\hbar} \\ \text{with} \qquad \hat{K}_\mathrm{F}[\tau_0](\tau+T) &= \hat{K}_\mathrm{F}[\tau_0](\tau) \ . \end{aligned} \tag{24}$$

The insight of Eq. 21 motivates us to look for a prudent choice of τ_0 that eliminates any explicit dependence of $\mathcal{H}_\mathrm{F}$ on τ_0. This is possible, following ref. [2], by absorbing all gauge dependence into new kick operators:

$$\mathcal{H}_\mathrm{eff} = e^{i\hat{K}(\tau_0)}\mathcal{H}_\mathrm{F}[\tau_0]e^{-i\hat{K}(\tau_0)} \tag{25}$$

which are related to the old ones via

$$e^{-i\hat{K}_\mathrm{F}[\tau_0](\tau)} = e^{-i\hat{K}(\tau)}e^{i\hat{K}(\tau_0)} \ . \tag{26}$$

Now, we can write down the Floquet theorem in its gauge-independent form

$$\mathcal{U}(\tau_f, \tau_i) = e^{-i\hat{K}(\tau_f)}e^{-i\mathcal{H}_\mathrm{eff}\times(\tau_f-\tau_i)/\hbar}e^{i\hat{K}(\tau_i)} \ . \tag{27}$$

(The second kick operator comes about because we do not want to fix the time-evolution to a particular starting time τ_0.) Eq. 27 gives the full time-evolution of an arbitrary state and can be interpreted as follows. First, we transform the starting state into a new frame of reference in which the Hamiltonian becomes time-independent using $e^{i\hat{K}(\tau_i)}$. Then, the time-evolution under the static Hamiltonian $\mathcal{H}_\mathrm{eff}$ takes place. Finally, the state is transformed again using $e^{-i\hat{K}(\tau_f)}$ which depends on the final time τ_f within one period T ('micromotion'). The Hamiltonian $\mathcal{H}_\mathrm{eff}$ is called 'effective Hamiltonian' and the operators $\hat{K}(\tau)$ are the 'non-stroboscopic kick operators' which, unlike $\hat{K}_\mathrm{F}[\tau_0](\tau)$ do not vanish at stroboscopic times τ_0, $2\tau_0$, etc.

Floquet's theorem can also be written as

$$\mathcal{H}_\mathrm{eff} = e^{i\hat{K}(\tau)}\hat{H}(\tau)e^{-i\hat{K}(\tau)} - i\hbar e^{i\hat{K}(\tau)}\left[\frac{\partial}{\partial\tau}e^{-i\hat{K}(\tau)}\right] \ , \tag{28}$$

which is equivalent to Eq. 27.

Floquet states and quasienergies

We want to make use of Floquet's theorem and calculate the time-evolution of an arbitrary state in the presence of an external, periodic drive ($\mathcal{H}(\tau) = \mathcal{H}(\tau + T)$).

Let us for the moment assume that we know the operator $\mathcal{U}(\tau_0+T,\tau_0) = e^{-i\mathcal{H}_\mathrm{F}\times T/\hbar}$ which evolves a state from one driving period to the next. Since the operator $\mathcal{U}(\tau_0+T,\tau_0)$ is unitary its eigenvalues are complex numbers that lie on the unit circle, allowing us to write its eigenvalues as $\{e^{-i\epsilon_n T/\hbar}\}$, which are called 'Floquet multipliers'. The notation $e^{-i\epsilon_n T/\hbar}$ reminds us that only the Floquet multipliers are uniquely defined, whereas the values $\{\epsilon_n\}$ are multi-valued, defined $\mod \hbar\omega$ with

$$\omega = \frac{2\pi}{T} \ . \tag{29}$$

Hence, the values $\{\epsilon_n \mod \hbar\omega\}$ are called 'quasienergies' (in analogy to the quasimomentum). Taking the multivaluedness of the energies ϵ_n into account, we can also directly get the eigenstates and eigenvalues via

$$\mathcal{H}_\mathrm{F}\,|n\rangle = \epsilon_n\,|n\rangle \ . \tag{30}$$

We should keep in mind that he eigenstates $\{|n\rangle\}$ of $\mathcal{U}(\tau_0+T,\tau_0)$ in reality carry the gauge dependence τ_0 and we should write $|n[\tau_0]\rangle$. However, we will now often omit the square brackets for clarity.

Now, we expand an arbitrary initial state $|\psi(\tau_0)\rangle$ in the eigenbasis of $\mathcal{U}(\tau_0+T,\tau_0)$

$$|\psi(\tau_0)\rangle = \sum_n |n\rangle \underbrace{\langle n|\psi(\tau_0)\rangle}_{\equiv a_n} \tag{31}$$

$$= \sum_n a_n\,|n\rangle \ . \tag{32}$$

Then, the state at later times will be

$$\begin{aligned} |\psi(\tau)\rangle &= \mathcal{U}(\tau,\tau_0)\,|\psi(\tau_0)\rangle \\ &\overset{(24)}{=} \sum_n a_n e^{-i\hat{K}_\mathrm{F}(\tau)} e^{-i\mathcal{H}_\mathrm{F}\times(\tau-\tau_0)/\hbar}\,|n\rangle \\ &= \sum_n a_n e^{-i\hat{K}_\mathrm{F}(\tau)} e^{-i\epsilon_n(\tau-\tau_0)/\hbar}\,|n\rangle \\ &= \sum_n a_n e^{-i\epsilon_n(\tau-\tau_0)/\hbar}\,|u_n(\tau)\rangle \ , \end{aligned} \tag{33}$$

where in Eq. 33 we have defined the 'Floquet modes'

$$|u_n(\tau)\rangle \equiv e^{-i\hat{K}_\mathrm{F}(\tau)}\,|n\rangle \tag{34}$$

$$\text{with } |u_n(\tau)\rangle \overset{(18)}{=} |u_n(\tau+T)\rangle \ . \tag{35}$$

In the literature, the states

$$|\psi_n(\tau)\rangle = e^{-i\epsilon_n(\tau-\tau_0)/\hbar}\,|u_n(\tau)\rangle \tag{36}$$

are often called 'Floquet states' in analogy with the Bloch theorem (Eq. 4). Again, the Floquet states $|\psi_n[\tau_0](\tau)\rangle$ and $|u_n[\tau_0](\tau)\rangle$ carry gauge dependence.

Equation 33 is the reward of all our previous derivation, giving the time-evolution of an arbitrary state $|\psi(\tau_0)\rangle$ as a function of time-independent coefficients a_n. In order words, in order to solve the time-dependent problem we need to find the Floquet Hamiltonian $\mathcal{H}_\mathrm{F}$ and the associated kick operator $\hat{K}_\mathrm{F}(\tau)$. Having diagonalised $\mathcal{H}_\mathrm{F}$ (or, more precisely, $\mathcal{U}(\tau_0+T,\tau_0)$), we can expand the initial state $|\psi(\tau_0)\rangle$ in eigenstates $|n\rangle$ with coefficients a_n and work out the Floquet modes $|u_n(\tau)\rangle$. Then, the time-evolution is directly given by Eq. 33. In particular, we have found the basis in which all time-dependence has been shifted into the basis states. The coefficients a_n do not depend on time, despite the periodic modulation in the Hamiltonian $\mathcal{H}(\tau)$. Thus, knowledge of the Floquet Hamiltonian $\mathcal{H}_\mathrm{F}$ allows us to treat the problem as if it was time-independent. This description is exact at stroboscopic times τ_0, τ_0+T, etc. since $|u_n[\tau_0](\tau_0)\rangle = |n[\tau_0]\rangle$, whereas at non-stroboscopic times we need to take special care of the Floquet modes (Eq. 34).

Example I: two-level system with circularly-polarised drive

The archetypical spin in a circularly-driven field is nice example in which the Floquet Hamiltonian can be simply written down. In this easy case, the kick operator does nothing else than going into the rotating frame.

We start with the Hamiltonian of a circularly driven spin-1/2:

$$\mathcal{H}_{\text{c-}1/2}(\tau) = \frac{\hbar\omega_0}{2}\sigma_z + \frac{\mu B_0}{2}\left(\sigma_x\cos\omega\tau + \sigma_y\sin\omega\tau\right) \ , \tag{37}$$

where σ_i are the Pauli matrices, ω_0 is the bare transition frequency, μ is the magnetic moment, B_0 is the magnetic field strength, and ω is the driving frequency. We transform the spin-1/2 Hamiltonian into the rotating frame using the kick operator

$$\hat{K}_\mathrm{F}[\tau_0](\tau) = -\frac{\omega(\tau-\tau_0)}{2}\times(\mathbb{1}-\sigma_z) \ . \tag{38}$$

Then, we have

$$\begin{aligned} \mathcal{H}_\mathrm{F}^\mathrm{c}[\tau_0] &= e^{i\hat{K}_\mathrm{F}[\tau_0](\tau)}\mathcal{H}_{\text{c-}1/2}(\tau)e^{-i\hat{K}_\mathrm{F}[\tau_0](\tau)} \\ &\quad - i\hbar e^{i\hat{K}_\mathrm{F}[\tau_0](\tau)}\left[\frac{\partial}{\partial\tau}e^{-i\hat{K}_\mathrm{F}[\tau_0](\tau)}\right] \\ &= \frac{\hbar\omega}{2}\mathbb{1} + \frac{\hbar}{2}(\omega_0-\omega)\sigma_z \\ &\quad + \frac{\mu B_0}{2}\left(\sigma_x\cos\omega\tau_0 + \sigma_y\sin\omega\tau_0\right) \end{aligned} \tag{39}$$

$$\Rightarrow\ \mathcal{H}_\mathrm{F}^\mathrm{c}[0] \overset{(\tau_0\equiv 0)}{=} \frac{\hbar\omega}{2}\mathbb{1} + \frac{\hbar}{2}(\omega_0-\omega)\sigma_z + \frac{\mu B_0}{2}\sigma_x \tag{40}$$

where we have chosen the Floquet gauge $\tau_0 = 0$ in the last line. The quasienergies are

$$\epsilon_\pm = \frac{\hbar}{2}\left(\omega \pm \sqrt{\Delta^2+\Omega_0^2}\right) \mod \hbar\omega \tag{41}$$

with $\Delta = \omega_0 - \omega$ and $\hbar\Omega_0 = \mu B_0$. The Floquet states can be evaluated according to Eq. 36.

Example II: two-level system with linearly-polarised drive

Only very few Floquet Hamiltonians can be directly computed as in the circularly driven spin-1/2 above. Our next example is the linearly-driven spin-1/2,

$$\mathcal{H}_{\text{lin-1/2}}(\tau) = \frac{\hbar\omega_0}{2}\sigma_z + \mu B_0 \sigma_x \cos\omega\tau \ , \tag{42}$$

which can be thought of as superposition of a left- and right-hand circularly polarised drive. It will retain some time-dependence after applying the transformation (Eq. 38) into the rotating frame since one of the two circular drives is 'rotated away' but the 'counter-rotating' one will oscillate twice the driving frequency. This time, we directly choose the Floquet gauge $\tau_0 = 0$:

$$\begin{aligned}\mathcal{H}^{\text{lin}}_{\text{rot}}[0](\tau) &= e^{i\hat{K}_{\text{F}}[0](\tau)}\mathcal{H}_{\text{lin-1/2}}(\tau)e^{-i\hat{K}_{\text{F}}[0](\tau)} \\ &\quad - i\hbar e^{i\hat{K}_{\text{F}}[0](\tau)}\left[\frac{\partial}{\partial\tau}e^{-i\hat{K}_{\text{F}}[0](\tau)}\right] \\ &\overset{\text{Ex}}{=} \mathcal{H}^{\text{c}}_{\text{F}}[0] + \frac{\mu B_0}{2}\left(\sigma_x\cos 2\omega\tau - \sigma_y \sin 2\omega\tau\right).\end{aligned} \tag{43}$$

It is evident from Eq. 43 that we require further assumptions to make progress in this situation. The answer will be to assume very high driving frequency $\omega \gg \mu B_0/2$ in order to neglect the 2ω terms in Eq. 43, such that the Hamiltonian reduces to $\mathcal{H}^{\text{c}}_{\text{F}}[0]$. This is the central idea behind the so-called 'high-frequency expansion'[3] of which you already know a prominent example: the famous rotating-wave approximation (RWA) in the linearly-driven two-level system.

III. HIGH-FREQUENCY EXPANSION

In almost all practical cases, it is impossible to find $\mathcal{H}_{\text{F}}$ or $\mathcal{H}_{\text{eff}}$ in a closed form. Instead, one can employ a high-frequency expansion (HFE)[4]

$$\mathcal{H}_{\text{eff}} = \sum_{n=0}^{\infty}\mathcal{H}^{(n)}_{\text{eff}} \ , \ \hat{K}(\tau) = \sum_{n=0}^{\infty}\hat{K}^{(n)}(\tau) \ , \tag{44}$$

in inverse powers of ω, i.e. $\mathcal{H}^{(n)}_{\text{eff}} \sim \omega^{-n}$ and $\hat{K}^{(n)}_{\text{eff}}(\tau) \sim \omega^{-n}$. Thus, the HFE is particularly useful if the driving frequency ω is much higher than all other energy scales, such that the series can be truncated.
We can expand the time-dependent $\mathcal{H}(\tau)$ in Fourier components

$$\mathcal{H}(\tau) = \sum_{l=-\infty}^{+\infty}\mathcal{H}_l e^{il\omega\tau} \ . \tag{45}$$

Then we find

$$\begin{aligned}\mathcal{H}^{(0)}_{\text{eff}} &= \frac{1}{T}\int_0^T \mathcal{H}(\tau)\mathrm{d}\tau \equiv \mathcal{H}_0 \\ \mathcal{H}^{(1)}_{\text{eff}} &= \frac{1}{\hbar\omega}\sum_{l=1}^{\infty}\frac{1}{l}[\mathcal{H}_l, \mathcal{H}_{-l}] \\ \mathcal{H}^{(2)}_{\text{eff}} &= \frac{1}{(\hbar\omega)^2}\left[\sum_{l=1}^{\infty}\frac{1}{2l^2}\left([[\mathcal{H}_l,\mathcal{H}_0],\mathcal{H}_{-l}] + [[\mathcal{H}_{-l},\mathcal{H}_0],\mathcal{H}_l]\right)\right. \\ &\quad \left. + \sum_{l,k=1}^{\infty}\frac{1}{3lk}\left([\mathcal{H}_l,[\mathcal{H}_k,\mathcal{H}_{-l-k}]] - [\mathcal{H}_l,[\mathcal{H}_{-k},\mathcal{H}_{k-l}]] + h.c.\right)\right]\end{aligned}$$

and

$$\hat{K}^{(0)} = 0 \tag{46}$$

$$\hat{K}^{(1)} = \frac{1}{i\hbar\omega}\sum_{l=1}^{\infty}\frac{1}{l}\left(\mathcal{H}_l e^{il\omega\tau} - \mathcal{H}_{-l}e^{-il\omega\tau}\right) \tag{47}$$

Example III: Bloch-Siegert shift

Now, using the high-frequency expansion we can tackle the linearly driven two-level system where we left off in example II. Our starting point is the Hamiltonian in the rotating frame (Eq. 43),

$$\mathcal{H}^{\text{lin}}_{\text{rot}}(\tau) = \frac{\hbar\Delta}{2}\sigma_z + \frac{\hbar\Omega_0}{2}\sigma_x + \frac{\hbar\Omega_0}{2}\left[\sigma_x\cos 2\omega\tau - \sigma_y\sin 2\omega\tau\right] \tag{48}$$

where we have chosen again $\tau_0 = 0$, neglecting global energy offsets. Applying the high-frequency expansion, we find

$$\mathcal{H}^{(0)}_{\text{eff}} = \mathcal{H}_0 = \frac{\hbar\Delta}{2}\sigma_z + \frac{\hbar\Omega_0}{2}\sigma_x \ \text{(RWA)} \tag{49}$$

$$\mathcal{H}^{(1)}_{\text{eff}} \overset{\text{Ex}}{=} \frac{\hbar\omega}{4}\left(\frac{\Omega_0}{\omega}\right)^2\sigma_z \ \text{(Bloch-Siegert)} \tag{50}$$

where $\mathcal{H}^{(1)}_{\text{eff}}$ is known as the Bloch-Siegert shift. We see that the first-order correction to the time-averaged Hamiltonian $\mathcal{H}_0$ becomes relevant for strong driving, i.e. $\Omega_0 \not\ll \omega$.

The high-frequency expansion is a good method to analytically derive effective Hamiltonians. In some cases, the correct choice of reference frame will make higher-order terms in the series expansion vanish and the resulting effective Hamiltonian becomes exact (exercise). If, however, the high-frequency expansion cannot easily be truncated, or the underlying Hamiltonian is too complicated, there are three other options to obtain the effective Hamiltonian numerically.

IV. NUMERICALLY SOLVING THE FLOQUET PROBLEM

In the following, we discuss three recipes to numerically calculate the effective Hamiltonian and/or the time-

evolution operator $\mathcal{U}(\tau_0+T,\tau_0)$.

Exact time-evolution of $\mathcal{U}(\tau_0+T,\tau_0)$

If the Hilbert space of $\mathcal{H}(\tau)$ is not too big, one can obtain $\mathcal{U}(\tau_0+T,\tau_0)$ by integrating the time-dependent Schrödinger equation over one period. First, expand the initial state in a certain basis

$$|\psi(\tau_0)\rangle = \sum_n c_n(\tau_0)\,|n\rangle \ . \tag{51}$$

Then, evolve $\psi(\tau_0)$ over one period according to the time-dependent Schrödinger equation

$$i\hbar\frac{\mathrm{d}}{\mathrm{d}\tau}c_n(\tau) = \sum_m \mathcal{H}_{nm}(\tau)c_m(\tau) \tag{52}$$

for each coefficient $c_n(\tau_0)$ from τ_0 to τ_0+T. The time-evolved vectors $\{c_n(\tau_0+T)\}$ directly give the columns of $\mathcal{U}(\tau_0+T,\tau_0)$ which, upon diagonalisation, give the Floquet multipliers $\{e^{-i\epsilon_n T/\hbar}\}$.

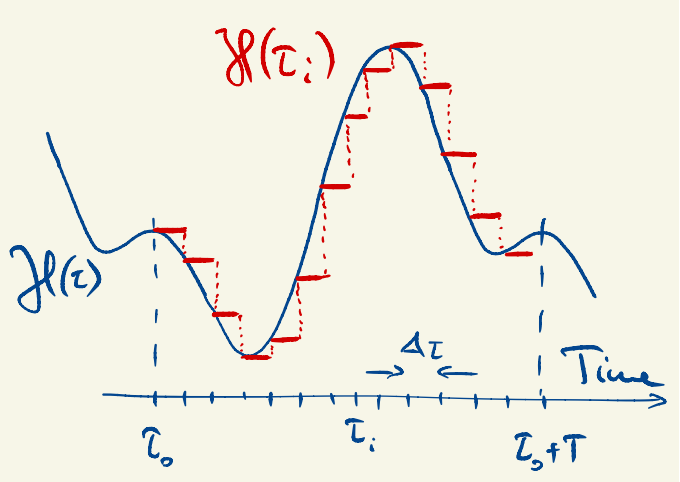

FIG. 5. Trotter decomposition of the time-evolution operator $\mathcal{U}(\tau_0+T,\tau_0)$. The time-axis is discretised in units of $\Delta\tau$, taking the Hamiltonian $\mathcal{H}(\tau_i)$ to be constant at each instant.

Trotter decomposition of $\mathcal{U}(\tau_0+T,\tau_0)$

If the Hilbert space is too large a numerical integration of Eq. 52 can become unfeasible. In this case, one can make use of the so-called Trotter decomposition of the time-evolution operator by dividing the timespan $[\tau_0,\tau_0+T]$ into N segments $\tau_i=\tau_0+i\Delta\tau$ with $\Delta\tau=T/N$:

$$\mathcal{U}(\tau_0+T,\tau_0) = \mathcal{T}\exp\left[-\frac{i}{\hbar}\int_{\tau_0}^{\tau_0+T}\mathcal{H}(\tau)\,\mathrm{d}\tau\right] \tag{53}$$

$$\simeq \exp\left[-\frac{i}{\hbar}\sum_{i=0}^{N-1}\mathcal{H}(\tau_i)\Delta\tau\right] \tag{54}$$

$$= \prod_{i=0}^{N-1}\exp\left[-\frac{i}{\hbar}\mathcal{H}(\tau_i)\Delta\tau\right] + \mathcal{O}\left(\Delta\tau^2\right)$$

Here, $\mathcal{T}$ denotes time-ordering and the third line is the Trotter decomposition, i.e. going from the exponential of a sum to the product of exponentials. Generally, this can be a hard problem, because Hamiltonians at different times do not commute, $[\mathcal{H}(\tau_i),\mathcal{H}(\tau_j)]\neq 0$. Trotter tells us that the error we make by ignoring the commutators is only $\mathcal{O}(\Delta\tau^2)$, i.e. it goes down quadratically with the duration of one time-step. During each time-step the Hamiltonian $\mathcal{H}(\tau_i)$ is taken to be constant, thus reducing the time-ordered integral to a product of exponentiated matrices, as illustrated in Fig. 5. As before, diagonalising $\mathcal{U}(\tau_0+T,\tau_0)$ gives the Floquet multipliers $e^{-i\epsilon_n T/\hbar}$.

The extended Hilbert space

Finally, we will discuss a method of obtaining the quasienergy spectrum via extending the Hilbert space by multiples of 'photon numbers' with $\hbar\omega$. More details about this method can be found in refs. [5, 6] (among others).

We start with the Floquet states from Eq. 36 which we expand in its harmonics due to the periodicity of the Floquet modes $|u_n(\tau)\rangle = |u_n(\tau+T)\rangle$ (c.f. Eq. 7 for Bloch waves).

$$|\psi_n(\tau)\rangle \ = \ e^{-i\epsilon_n\tau/\hbar}\,|u_n(\tau)\rangle \tag{55}$$

$$\overset{(35)}{=} e^{-i\epsilon_n\tau/\hbar}\sum_{m=-\infty}^{+\infty} e^{-im\omega\tau}\,|n,m\rangle \ , \tag{56}$$

where $|n,m\rangle$ are the Fourier-coefficients of $|u_n(\tau)\rangle$ and we have again dropped the explicit dependence on the starting time τ_0. Plugging this ansatz into the time-dependent Schrödinger equation (Eq. 1) yields

$$(\epsilon_n+m\hbar\omega)\,|n,m\rangle \overset{\text{Ex}}{=} \sum_{m'=-\infty}^{+\infty}\mathcal{H}_{m-m'}\,|n,m'\rangle \ . \tag{57}$$

As before, the $\mathcal{H}_l$ are the Fourier-components of the time-dependent Hamiltonian $\mathcal{H}(\tau)$ (Eq. 45). Here, we have created an over-complete problem, as the ϵ_n are only defined $\mod \hbar\omega$. The multi-valuedness of ϵ_n is the reason why we obtain an extended Hilbert space and the solutions to Eq. 57 will be $\hbar\omega$-periodic. We can write Eq. 57 explicitly as

$$\begin{pmatrix} \ddots & \mathcal{H}_{-1} & \mathcal{H}_{-2} & & \\ \mathcal{H}_1 & \mathcal{H}_0 - m\hbar\omega & \mathcal{H}_{-1} & \mathcal{H}_{-2} & \\ \mathcal{H}_2 & \mathcal{H}_1 & \mathcal{H}_0 - (m+1)\hbar\omega & \mathcal{H}_{-1} & \\ & \mathcal{H}_2 & \mathcal{H}_1 & \ddots & \end{pmatrix} \begin{pmatrix} \vdots \\ |n,m\rangle \\ |n,m+1\rangle \\ \vdots \end{pmatrix} = \epsilon_n \begin{pmatrix} \vdots \\ |n,m\rangle \\ |n,m+1\rangle \\ \vdots \end{pmatrix} \tag{58}$$

Note that the big matrix in Eq. 58 consists of many blocks à $d \times d$ entries, where d is the dimension of the Hilbert space of $\mathcal{H}(\tau)$. Likewise, the vectors $|n,m\rangle$ are d-dimensional.

For a common time-dependent Hamiltonian of the kind

$$\mathcal{H}(\tau) = \mathcal{H}_0 + Ve^{i\omega\tau} + V^\dagger e^{-i\omega\tau} \tag{59}$$

the extended-space Hamiltonian takes the simple form

$$\begin{pmatrix} \ddots & V & 0 & & \\ V^\dagger & \mathcal{H}_0 + \hbar\omega & V & 0 & \\ 0 & V^\dagger & \mathcal{H}_0 & V & 0 \\ & 0 & V^\dagger & \mathcal{H}_0 - \hbar\omega & V \\ & & 0 & V^\dagger & \ddots \end{pmatrix}, \tag{60}$$

similar to a tight-binding Hamiltonian with nearest-neighbour hopping. Since the periodic drive often has the cosine-shape of Eq. 59, the numerical evaluation of this block-diagonal matrix can be very efficient. But how can we truncate this matrix which is in general infinite-dimensional? Here, we have to distinguish two regimes. In the weak driving regime, i.e. $\hbar\omega \gg \langle V \rangle$, which is equivalent to the high-frequency regime, only one block of this Hamiltonian is relevant, e.g.

$$\begin{pmatrix} \mathcal{H}_0 + \hbar\omega & V \\ V^\dagger & \mathcal{H}_0 \end{pmatrix}, \tag{61}$$

in which we recognise the rotating-wave approximation (Eq. 49 for the spin-1/2). If instead the driving frequency is on the same order as the time-dependent Hamiltonian $\hbar\omega \sim \langle V \rangle$, we reach the 'strong-driving' limit in which many blocks have to be taken into account.

V. FLOQUET ENGINEERING WITH OPTICAL LATTICES

Now we will bring together the two concepts, Bloch theory and Floquet theory, giving spatio-temporal 'Floquet-Bloch waves'.

Lattice shaking: reference frames and energy scales

Before we start tackling the Hamiltonian, we want to choose a convenient frame of reference in which to describe the problem.

A common experimental method to implement lattice shaking schemes employs a piezo-electric actuator to move the retro-reflecting mirror that defines the standing wave. In this way, the position of the optical lattice $V_{\text{lat}}(x)$ can be modulated in time with a waveform $x_m(\tau)$. Another way to generate the shaken lattice is to modulate the frequency of one of the two beams that form the standing wave, resulting in time-periodic phase-shift on the light.

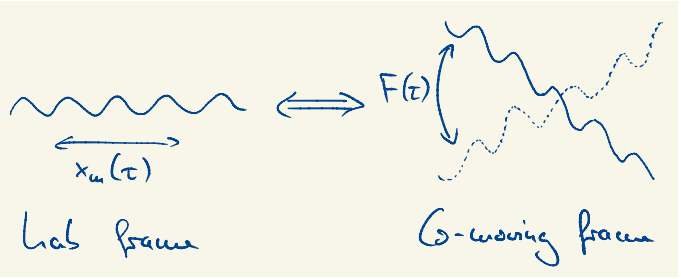

FIG. 6. The moving lattice in the lab frame (left) can be transformed into an oscillating force (right) in the co-moving frame.

A generic hamiltonian describing these situations is

$$\mathcal{H}_{\text{lab}}(\tau) = \frac{\hat{p}^2}{2m} + V_{\text{lat}}[\hat{x} - x_m(\tau)] \,. \tag{62}$$

We consider the unitary transformation $\mathcal{R}_0(\tau) = e^{-i\hat{p}x_m(\tau)/\hbar}$ and apply $\mathcal{R}_0^\dagger(\tau)$ to $\mathcal{H}_{\text{lab}}$ according to

$$\tilde{\mathcal{H}}(\tau) = \mathcal{R}(\tau)\mathcal{H}(\tau)\mathcal{R}^\dagger(\tau) + i\hbar\left[\frac{\partial}{\partial\tau}\mathcal{R}(\tau)\right]\mathcal{R}^\dagger(\tau) \,. \tag{63}$$

with $\mathcal{R}(\tau) = \mathcal{R}_0^\dagger(\tau)$, using

$$e^A B e^{-A} = B + [A,B] + \frac{1}{2!}[A,[A,B]] + \ldots \tag{64}$$

to get

$$\mathcal{H}_{\text{rot}}(\tau) = \frac{[\hat{p} - A(\tau)]^2}{2m} + V_{\text{lat}}(\hat{x}) \tag{65}$$

(neglecting a non-operator valued term involving $A(\tau)^2$, which can be transformed away with another transformation). This frame of reference is called the rotating frame. We read off the 'vector potential' $A(\tau) = m\dot{x}_m(\tau)$. Now, we apply a second unitary transformation $\mathcal{R}_1(\tau) = e^{-i\hat{x}A(\tau)/\hbar}$ to reach the reference frame that is co-moving with the shaken lattice:

$$\mathcal{H}_{\text{cm}}(\tau) = \frac{\hat{p}^2}{2m} + V_{\text{lat}}(\hat{x}) - F(\tau)\hat{x} \tag{66}$$

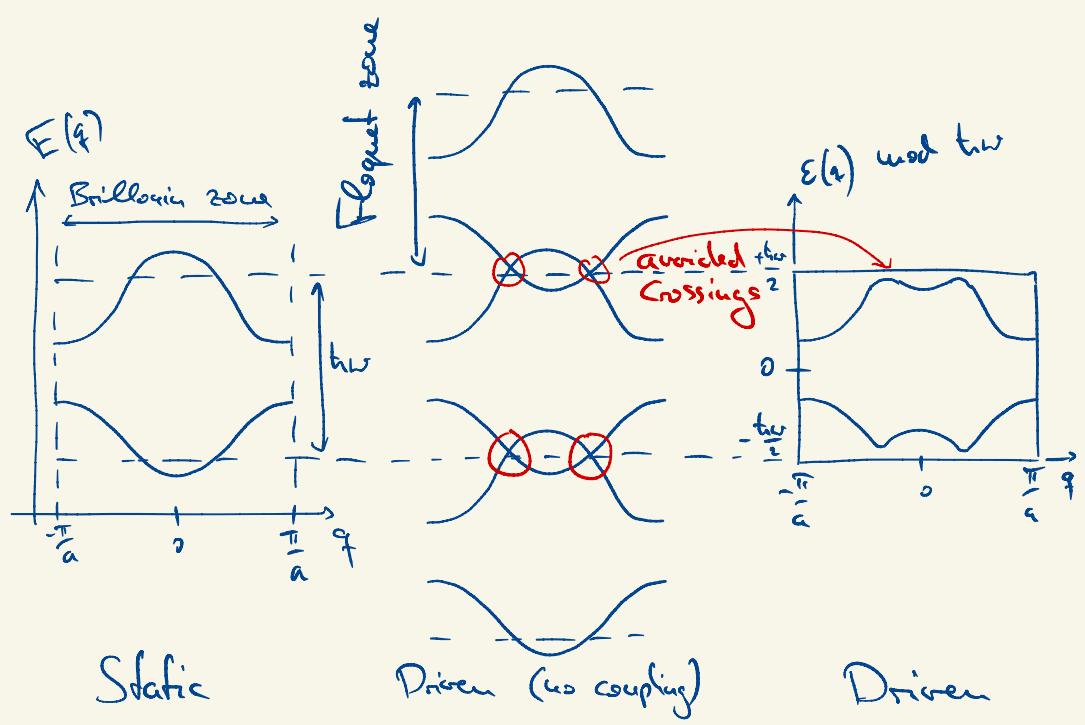

FIG. 7. Resonant coupling of two Bloch bands. Left: static system. The dispersion has two bands which are not coupled in the absence of any driving. Middle: driven system with infinitesimal driving amplitude. The dispersion relation is extended by multiples of $\hbar\omega$. Right: driven system with non-zero driving amplitude. The dispersion is folded back into a single Floquet-zone, with interband couplings appearing where two bands used to cross. When the driving frequency ω is on the same order as the band separation the two bands (say, 'valence band' and 'conduction band') become hybridised.

with the time-periodic force $F(\tau) = -m\ddot{x}_m = -\dot{A}(\tau)$, as shown in Fig. 6. The co-moving frame (Eq. 66) is particularly useful when describing the optical lattice as tight-binding model (Exercise).

Driven two-band system

As a first example, we will only consider two Bloch bands (e.g. a two-site tight-binding model) in which we introduce a resonant driving at the frequency of the band separation (Fig. 7). The resulting Floquet-Bloch dispersion can be calculated using any of the formalisms introduce above (section IV).

Shaken optical lattice

Using the shaking waveform

$$x_m(\tau) = x_0 \cos(\omega\tau) \tag{67}$$
$$A(\tau) = m\dot{x}_m(\tau) = -mx_0\omega \sin(\omega\tau) \tag{68}$$

in the lab frame (67), or in the rotating frame (68), we can study the full optical lattice problem, including higher bands. The moving-lattice potential in the lab frame reads

$$V(\hat{x}, \tau) = V_0 \cos^2\left[k_{\text{lat}}\left(\hat{x} - x_m(\tau)\right)\right] \ , \tag{69}$$

leading to the time-dependent Hamiltonian (in the rotating frame)

$$\mathcal{H}_{l,l'}(\tau) = \begin{cases} \frac{\hbar^2}{2m}(q + 2lk_{\text{lat}} - A(\tau)/\hbar)^2 & \text{for} \quad l = l' \\ V_0/4 & \text{for} \quad |l - l'| = 1 \\ 0 & \text{otherwise,} \end{cases}$$

as in Eq. 9 in the beginning. It is convenient to introduce the dimensionless shaking amplitude

$$K_0 \overset{\text{Ex}}{=} \frac{mx_0\omega d}{\hbar} \ . \tag{70}$$

The resulting Floquet-Bloch bandstructure is shown in Fig. 8, taken from ref. [7] for three different values of K_0. They can be calculated numerically using the Trotter decomposition (or the exact time-evolution method).

Dynamical localisation

Several experiments have realised the flattening of the lowest Floquet-Bloch band, giving rise to the phenomenon of 'dynamical localisation' [8]. As you will calculate in the exercise, the flattening occurs around the

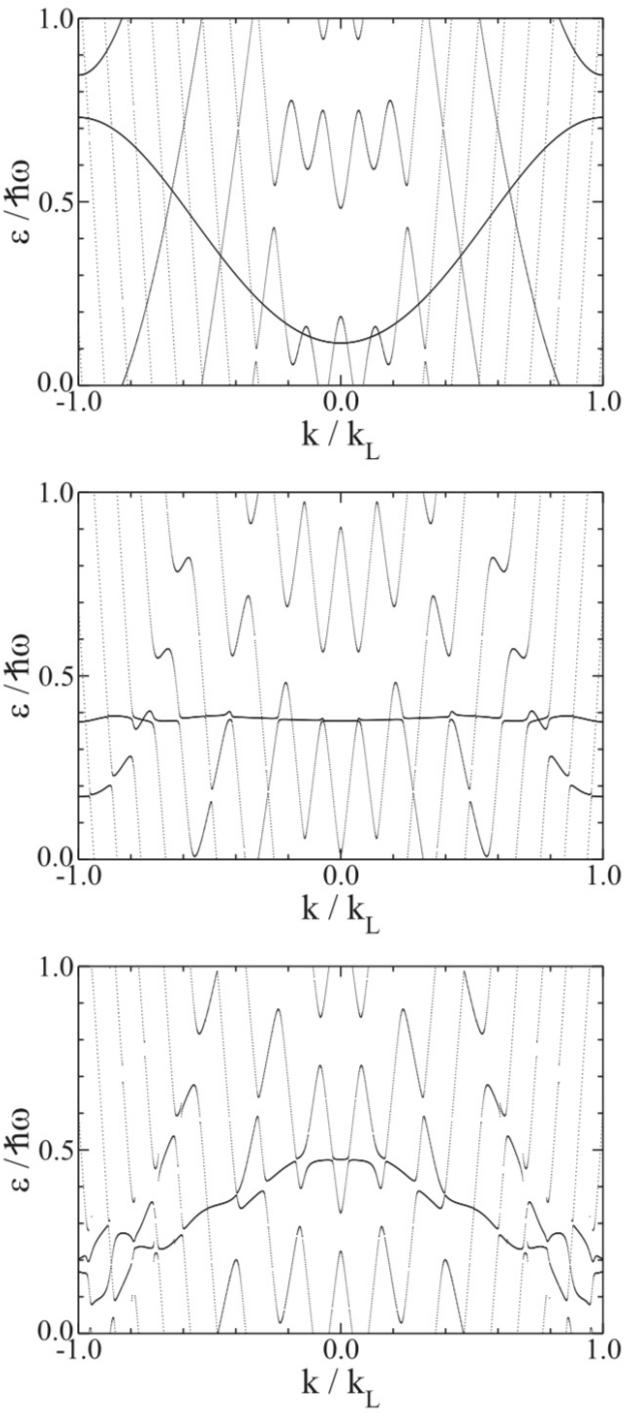

FIG. 8. Floquet-Bloch bands for $V_0 = 4E_{\rm rec}$, $\hbar\omega = 0.5E_{\rm rec}$, and $K_0 = [0.20, 0.74, 1.21] \times \pi$ (top to bottom). The driving frequency is chosen higher than the bandwidth of the lowest band, but lower than the first band gap. Consequently, the lowest band stays mostly intact, but the higher bands become hybridised for low driving strengths ($K_0 = 0.2\pi$). The shape of the lowest band is changed significantly by the off-resonant driving, it becomes flat (middle) and inverted (bottom), albeit with many couplings to higher bands. These crossings can be avoided by increasing the separation of the bands (deeper lattices) [7]. In their definition, $k_{\rm L} = \pi/a$.

zero of the zeroth Bessel function $\mathcal{J}_0(K_0)$, which is also reflected in the full calculation in Fig. 8. The rescaling of the tunnelling with the zeroth Bessel function is the fundamental manifestation of off-resonant lattice shaking.

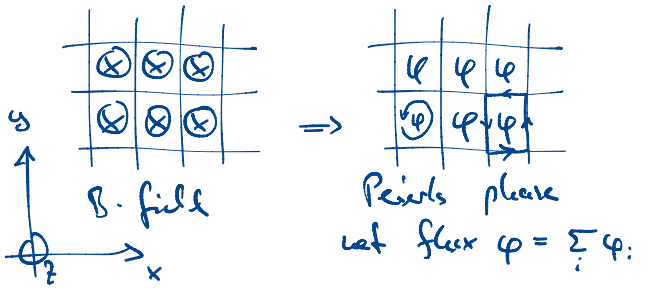

FIG. 9. The action of the real magnetic field on a tight-binding lattice.

Artificial magnetic fields

Arguably the most important application of Floquet theory in optical lattices is the generation of artificial magnetic fields. The two ingredients required to achieve an artificial magnetic field is the breaking of time-reversal symmetry, on the one hand, and a non-trivial distribution of tunnellings in the lattice, on the other. There is an excellent review on this topic by Cooper *et al.* [9].

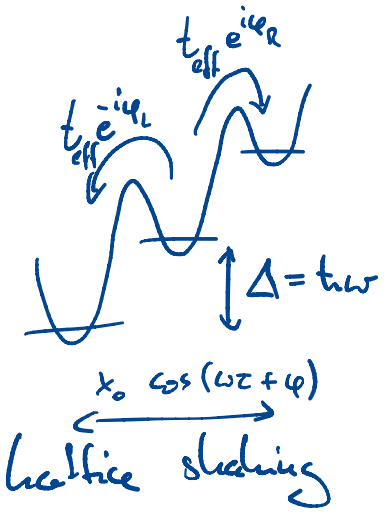

FIG. 10. Induced Peierls phases φ_R in a resonantly-shaken optical lattice.

Let us first consider the action of a uniform magnetic field on a lattice, as depicted in Fig. 9. In the tight-binding model it shows up as complex tunnelling matrix elements that add up to a constant value φ, called magnetic flux, when hopping around a unit cell. The

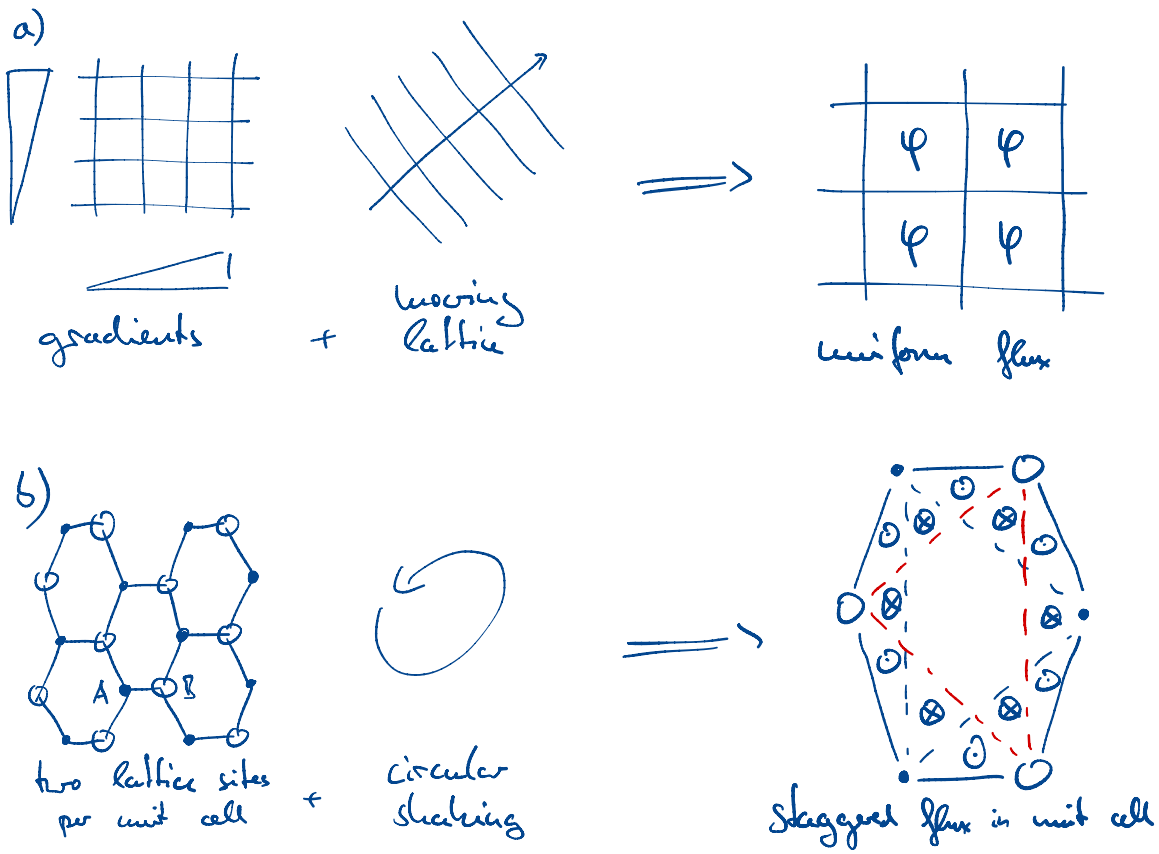

FIG. 11. Generating an artificial magnetic field in an optical lattice. Method a) employs a non-uniform distribution of Peierls phase factors in order to achieve a net uniform flux. A secondary, moving optical lattice leads to a periodic modulation of the on-site energies of the lattice. The frequency of this modulation is chosen to be resonant with a static tilt in both x- and y-directions. Method b) uses circular lattice shaking in order to induce next-nearest-neighbour tunnellings. The shaking frequency can be chosen resonant with a large AB-sublattice offset or it can be off-resonant. While hopping around the entire unit cell does not lead to a magnetic flux, individual paths within the unit cell do. This pattern of staggered fluxes was first proposed by Haldane [10] in 1988 and it was later realised in the laboratory using ultracold atoms.

argument φ_i of each complex tunnelling is called Peierls phase,

$$t_i = |t_i| e^{i\varphi_i} \tag{71}$$

$$\sum_{i=1}^{4} \varphi_i = \varphi \ . \tag{72}$$

As you will show in the exercise, non-zero Peierls phases can be engineered via lattice shaking. For example, resonant shaking with a static tilt Δ in the lattice gives rise to a complex tunnelling element, as shown schematically in Fig. 10.

However, it is clear from Fig. 10 that simply adding a tilt, even in a two-dimensional lattice, will not result in a net flux φ, as hopping in the opposite direction cancels the phase of hopping in the forward direction. Therefore, a more complicated Peierls phase structure must be engineered in order to achieve a non-zero flux. Two possible options of doing this are sketched in Fig. 11.

[1] Marin Bukov, Luca D'Alessio, and Anatoli Polkovnikov, "Universal high-frequency behavior of periodically driven systems: from dynamical stabilization to Floquet engineering," Advances in Physics **64**, 139–226 (2015).

[2] N. Goldman and J. Dalibard, "Periodically Driven Quantum Systems: Effective Hamiltonians and Engineered Gauge Fields," Physical Review X **4**, 31027 (2014).

[3] Or the 'Floquet-Magnus expansion' in the stroboscopic case.

[4] The analogous expressions for $\mathcal{H}_{\mathrm{F}}$, called 'Floquet-Magnus' expansion, can be found in ref. [1], together with higher-order terms of the expansions.

[5] Jean Dalibard, "Réseaux dépendant du temps," Collège de France, Cours 4 (2013).

[6] Mark S. Rudner and Netanel H. Lindner, *The Floquet Engineer's Handbook*, Vol. 2003.08252 (arXiv, 2020).

[7] Martin Holthaus, "Floquet engineering with quasienergy bands of periodically driven optical lattices," Journal of Physics B: Atomic, Molecular and Optical Physics **49**, 013001 (2016).

[8] H. Lignier, C. Sias, D. Ciampini, Y. Singh, A. Zenesini, O. Morsch, and E. Arimondo, "Dynamical Control of Matter-Wave Tunneling in Periodic Potentials," Physical Review Letters **99** (2007), 10.1103/PhysRevLett.99.220403.

[9] N. R. Cooper, J. Dalibard, and I. B. Spielman, "Topological bands for ultracold atoms," Reviews of Modern Physics **91** (2019), 10.1103/RevModPhys.91.015005.

[10] F. D. M. Haldane, "Model for a Quantum Hall Effect without Landau Levels: Condensed-Matter Realization of the "Parity Anomaly"," Physical Review Letters **61**, 2015–2018 (1988).